Anisotropic Flow of Charged Particles in Pb-Pb Collisions at root S-NN=5.02 TeV

Adam, J.

2016-04-01

Anisotropic Flow of Charged Particles in Pb-Pb Collisions at $\sqrt{s_{NN}} = 5.02$ TeV

J. Adam *et al.**
(The ALICE Collaboration)
(Received 4 February 2016; published 1 April 2016)

We report the first results of elliptic (v_2), triangular (v_3), and quadrangular (v_4) flow of charged particles in Pb-Pb collisions at a center-of-mass energy per nucleon pair of $\sqrt{s_{NN}} = 5.02$ TeV with the ALICE detector at the CERN Large Hadron Collider. The measurements are performed in the central pseudorapidity region $|\eta| < 0.8$ and for the transverse momentum range $0.2 < p_T < 5$ GeV/c. The anisotropic flow is measured using two-particle correlations with a pseudorapidity gap greater than one unit and with the multiparticle cumulant method. Compared to results from Pb-Pb collisions at $\sqrt{s_{NN}} = 2.76$ TeV, the anisotropic flow coefficients v_2, v_3, and v_4 are found to increase by $(3.0 \pm 0.6)\%$, $(4.3 \pm 1.4)\%$, and $(10.2 \pm 3.8)\%$, respectively, in the centrality range 0%–50%. This increase can be attributed mostly to an increase of the average transverse momentum between the two energies. The measurements are found to be compatible with hydrodynamic model calculations. This comparison provides a unique opportunity to test the validity of the hydrodynamic picture and the power to further discriminate between various possibilities for the temperature dependence of shear viscosity to entropy density ratio of the produced matter in heavy-ion collisions at the highest energies.

The goal of studies with relativistic heavy-ion collisions is to investigate the quark-gluon plasma (QGP), a state of matter where quarks and gluons move freely over distances that are large in comparison to the typical size of a hadron. The transition from normal nuclear matter to the QGP state is expected to occur at extreme values of energy density (0.2–0.5 GeV/fm^3, according to lattice quantum chromodynamics calculations [1,2]), which are accessible in ultrarelativistic heavy-ion collisions at the Large Hadron Collider (LHC) [3,4]. The study of such collisions provides a unique opportunity to probe the properties of the QGP in a region of the QCD phase diagram where a crossover between the deconfined phase and normal nuclear matter is expected [5–9].

Studies of the azimuthal anisotropy of particle production have contributed significantly to the characterization of the system created in heavy-ion collisions [10,11]. Anisotropic flow, which measures the momentum anisotropy of the final-state particles, is sensitive both to the initial geometry of the overlap region and to the transport properties and equation of state of the system. By using a general Fourier series decomposition of the azimuthal distribution of produced particles,

$$\frac{dN}{d\varphi} \propto 1 + 2 \sum_{n=1}^{\infty} v_n \cos[n(\varphi - \Psi_n)], \qquad (1)$$

anisotropic flow is quantified with coefficients v_n and corresponding symmetry planes Ψ_n [12]. Because of the approximately ellipsoidal shape of the overlap region in noncentral heavy-ion collisions (i.e., collisions that correspond to a large impact parameter), the dominant flow coefficient is v_2, referred to as elliptic flow. In the transition from highest RHIC to LHC energies, elliptic flow increases by 30% [13], as predicted by hydrodynamic models that include viscous corrections [14–18]. Nonvanishing values of higher anisotropic flow harmonics v_3–v_6 at the LHC are ascribed primarily to the response of the produced QGP to fluctuations of the initial energy density profile of the colliding nucleons [19–22]. Moreover, because of such fluctuations, each flow harmonic v_n has a distinct symmetry plane Ψ_n and recent measurements of their intercorrelations provide independent constraints on the QGP properties [23]. The combination of all such results demonstrates that the shear viscosity to entropy density ratio (η/s) of the QGP produced in ultrarelativistic heavy-ion collisions at RHIC and LHC has a value close to $1/4\pi$, a lower bound obtained in strong-coupling calculations based on the AdS/CFT conjecture [24].

Recently, predictions from Niemi *et al.* on anisotropic flow coefficients for Pb–Pb $\sqrt{s_{NN}} = 5.02$ TeV collisions using the Eskola-Kajantie-Ruuskanen-Tuominen model were reported in Ref. [25]. These predictions have a special emphasis on the discriminating power between various parametrizations of the temperature dependence of η/s. It was argued that in the transition from 2.76 to 5.02 TeV, the elliptic flow estimated from two-particle correlations (denoted further in the text as $v_2\{2\}$, where the number in the curly brackets indicates the number of particles that

*Full author list given at the end of the article.

are used in correlation [26]) can increase, at most, ∼5% for all centrality classes. Details of the increase depend on the parametrization of $\eta/s(T)$. On the other hand, higher flow harmonic observables, like $v_3\{2\}$ and $v_4\{2\}$, are predicted to increase more rapidly, 10%–30%. With a different approach, where previously measured values of flow harmonics at lower LHC energies are taken as a baseline, Noronha-Hostler *et al.* [27] predict a larger increase for both elliptic and triangular flow in peripheral compared to central collisions in transition from 2.76 to 5.02 TeV. They conclude that the anisotropic flow already reaches saturation and its maximum value in central collisions at 2.76 TeV.

A necessary condition for the development of anisotropic flow is the initial anisotropy in the interaction region of the two colliding ions. These coordinate space anisotropies are described in terms of eccentricities, which are not directly accessible experimentally. Nonetheless, the theoretical modeling of such eccentricities is actively being studied. For instance, hydrodynamic calculations based on a MC-Glauber model and MC–Kharzeev-Levin-Nardi initial conditions do not agree on the details of the saturation of elliptic flow at LHC energies [28]. However, with these two initial state models, it was shown that the final spatial eccentricity decreases monotonically as the collision energy increases [28], and is expected to become negative only at the very large collision energies available at the LHC (see Fig. 9 in Ref. [28]).

In addition to the initial conditions, various other stages of evolution of the system in a heavy-ion collision may contribute to the development of anisotropic flow. At lower energies, the state of the system will primarily resemble a hadronic gas, and hadron rescattering is the dominant contribution to the anisotropic flow. At higher energies, anisotropic flow mostly develops in the thermalized color-deconfined QGP phase. However, even at these higher energies, the contribution from the hadronic phase can be significant. The relative amount of time the system spends in different phases varies with collision energy [28,29]. Radial flow, a measure for the average velocity of the system's collective radial expansion, also increases as a function of collision energy, which translates into more particles being transferred to a higher transverse momentum (p_T) region, thus leading to an increase in average anisotropic flow values. On the other hand, the opposite dependence of differential $v_2(p_T)$ is expected for light (an increase at low p_T) and heavy particles (a decrease at low p_T) as a function of collision energy, which might yield to the saturation of the elliptic flow signal [28]. Finally, the relative importance of various stages in the system evolution as a function of collision energy can also vary for each flow coefficient [29].

The data used in this Letter were recorded with the ALICE detector [30,31] in November 2015 in run 2 at the LHC with Pb-Pb collisions at $\sqrt{s_{NN}} = 5.02$ TeV. Minimum

bias Pb–Pb events were triggered by the coincidence of signals from the V0 detector. The V0 detector is composed of two arrays of scintillator counters, V0-A and V0-C, which cover the pseudorapidity ranges $2.8 < \eta < 5.1$ and $-3.7 < \eta < -1.7$, respectively [30]. Centrality quantifies the fraction of a geometrical cross section of the colliding nuclei. It is determined using the sum of the amplitudes of the V0-A and -C signals, which provides a resolution better than 0.5% and up to 20% for central Pb-Pb collisions, and better than 2% for peripheral collisions [32]. The off-line event selection employs the information from two zero degree calorimeters (ZDCs) [30] positioned 112.5 m from the interaction point on either side. Beam background events are removed using timing information from the V0 and the ZDCs, respectively. To ensure a uniform acceptance and reconstruction efficiency in the pseudorapidity region $|\eta| < 0.8$, only events with a reconstructed vertex within 10 cm from the center of the detector along the beam direction were used. A sample of 140 k Pb-Pb collision events passed the selection criteria. Only one low luminosity run (with a trigger rate of 27 Hz) was used, being least affected by pileup and distortions from space charge in the main tracking detector, the time projection chamber (TPC).

Charged tracks are reconstructed using the ALICE inner tracking system (ITS) and the TPC [30]. This combination ensures a high detection efficiency, optimum momentum resolution, and a minimum contribution from photon conversions and secondary charged particles produced either from the detector material or from weak decays. In order to reduce the contamination from secondary particles, only tracks with a distance of closest approach to the interaction point of less than 3 cm, both in the longitudinal and transverse directions, are accepted. The tracking efficiency is calculated from a Monte Carlo simulation that uses HIJING [33] to simulate particle production. GEANT3 [34] is then used for transporting simulated particles, followed by a full calculation of the detector response (including the production of secondary particles) and track reconstruction performed with the ALICE reconstruction framework. The tracking efficiency is ∼70% at $p_T \sim 0.2$ GeV/c and increases to an approximately constant value of ∼80% for $p_T > 1$ GeV/c. The p_T resolution is better than 5% for the region presented in this Letter. The systematic uncertainty related to the nonuniform reconstruction efficiency was found to be at the level of 1%. The flow coefficients from tracks that are reconstructed from TPC space points alone were compared to coefficients extracted from particles that used both TPC clusters and ITS hits, which were found to agree within ∼2%. This difference was taken into account in the estimation of the systematic uncertainty. Altering the selection criteria for the tracks reconstructed with the TPC resulted in a variation of the results of 0.5%, at most. Other selection criteria that have been scrutinized are the

centrality determination, e.g., using the silicon pixel detector (SPD), which contributed by less than 1%, the polarity of the magnetic field of the ALICE detector and the position of the reconstructed primary vertex, whose contributions were found to be negligible. The systematic uncertainties evaluated for each of the sources mentioned above were added in quadrature to obtain the total systematic uncertainty of the measurements.

In this Letter, we report the anisotropic flow measurements obtained from two- and multiparticle cumulants, using the approach proposed in Refs. [35–37]. These two measurements have different sensitivities to flow fluctuations and nonflow effects. Nonflow effects are azimuthal correlations not associated with the symmetry planes and usually arise from resonance decays and jets. Their contributions are expected to be suppressed when using a large pseudorapidity gap between particle pairs. Thus, in this study, we require a pseudorapidity gap of $|\Delta\eta| > 1$. This observable is denoted as $v_n\{2, |\Delta\eta| > 1\}$. On the other hand, nonflow contributions to multiparticle cumulants $v_n\{4\}$, $v_n\{6\}$, $v_n\{8\}$ are found to be negligible in events with large multiplicities characteristic of heavy-ion collisions [38].

Figure 1(a) presents the centrality dependence of v_2, v_3, and v_4 from two- and multiparticle cumulants, integrated over the p_T range $0.2 < p_T < 5.0$ GeV/c, for 2.76 and 5.02 TeV Pb-Pb collisions. To elucidate the energy evolution of v_2, v_3, and v_4, the ratios of anisotropic flow measured at 5.02 to 2.76 TeV are presented in Figs. 1(b) and 1(c). Assuming that nonflow effects are suppressed by the pseudorapidity gap, the remaining differences between two- and multiparticle cumulants of v_2 can be related to the strength of elliptic flow fluctuations, which are expected to give a positive and a negative contribution to the two- and multiparticle cumulant estimates, respectively [11]. Moreover, the multiparticle cumulants $v_2\{4\}$, $v_2\{6\}$, and $v_2\{8\}$ are all observed to agree within 1%, which indicates that nonflow effects are largely suppressed. It is seen that $v_2\{2, |\Delta\eta| > 1\}$ increases from central to peripheral collisions and reaches a maximum value of 0.104 ± 0.001 (stat) ± 0.002 (syst) in the 40%–50% centrality class. For the higher harmonics, i.e., v_3 and v_4, the values are smaller and the centrality dependence is much weaker.

Furthermore, the predictions of anisotropic flow coefficients v_n from the previously mentioned hydrodynamic model [27] are compared to the measurements in Fig. 1(a). These predictions combine the changes in initial spatial anisotropy and the hydrodynamic response (treated as systematic uncertainty and shown by the width of the bands). The predictions are compatible with the measured anisotropic flow v_n coefficients. At the same time, a different hydrodynamic calculation [25], which employs both constant $\eta/s = 0.20$ and temperature dependent η/s, can also describe the increase in anisotropic flow
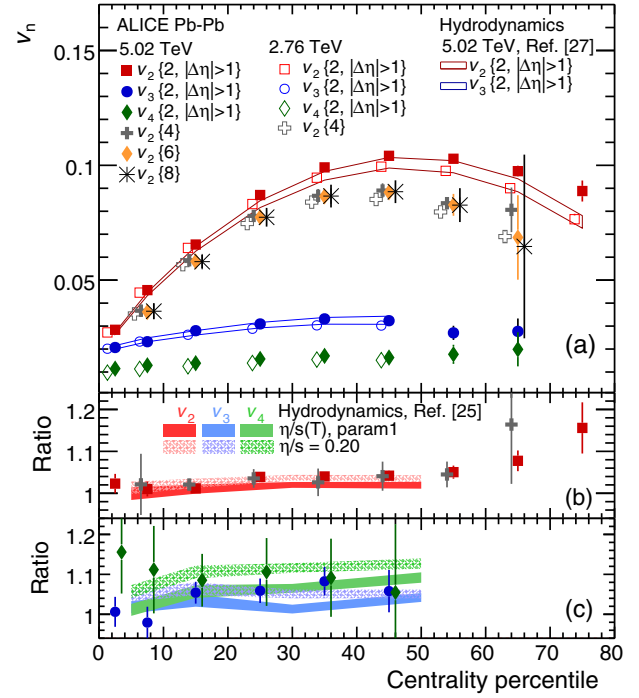

FIG. 1.   (a) Anisotropic flow v_n integrated over the p_T range $0.2 < p_T < 5.0$ GeV/c, as a function of event centrality, for the two-particle (with $|\Delta\eta| > 1$) and multiparticle cumulant methods. Measurements for Pb-Pb collisions at $\sqrt{s_{NN}} = 5.02$ (2.76) TeV are shown by solid (open) markers [20]. The ratios of $v_2\{2, |\Delta\eta| > 1\}$ (red), $v_2\{4\}$ (gray) and $v_3\{2, |\Delta\eta| > 1\}$ (blue), $v_4\{2, |\Delta\eta| > 1\}$ (green) between Pb-Pb collisions at 5.02 and 2.76 TeV are presented in Figs. 1(b) and 1(c). Various hydrodynamic calculations are also presented [25,27]. The statistical and systematical uncertainties are summed in quadrature (the systematic uncertainty is smaller than the statistical uncertainty, which is typically within 5%). Data points are shifted for visibility.

measurements of v_2 [shown in Fig. 1(b)], v_3 and v_4 [see Fig. 1(c)]. In particular, among the different scenarios proposed in Ref. [25], the measurements seem to favor a constant η/s going from $\sqrt{s_{NN}} = 2.76$ to 5.02 TeV Pb-Pb collisions.

The increase of v_2 and v_3 from the two energies is rather moderate, while for v_4 it is more pronounced. In addition, none of the ratios of flow harmonics exhibit a significant centrality dependence in the centrality range 0%–50%, and thus the results of a fit with a constant value over these ratios are reported. An increase of $(3.0 \pm 0.6)\%$, $(4.3 \pm 1.4)\%$, and $(10.2 \pm 3.8)\%$ is obtained for elliptic, triangular, and quadrangular flow, respectively, over the centrality range 0%–50% in Pb-Pb collisions when going from 2.76 to 5.02 TeV. This increase of anisotropic flow is compatible with theoretical predictions described in Refs. [25,27]. Overall, these measurements support a low value of η/s for the system created in Pb-Pb collisions at $\sqrt{s_{NN}} = 5.02$ TeV and seem to indicate that it does not
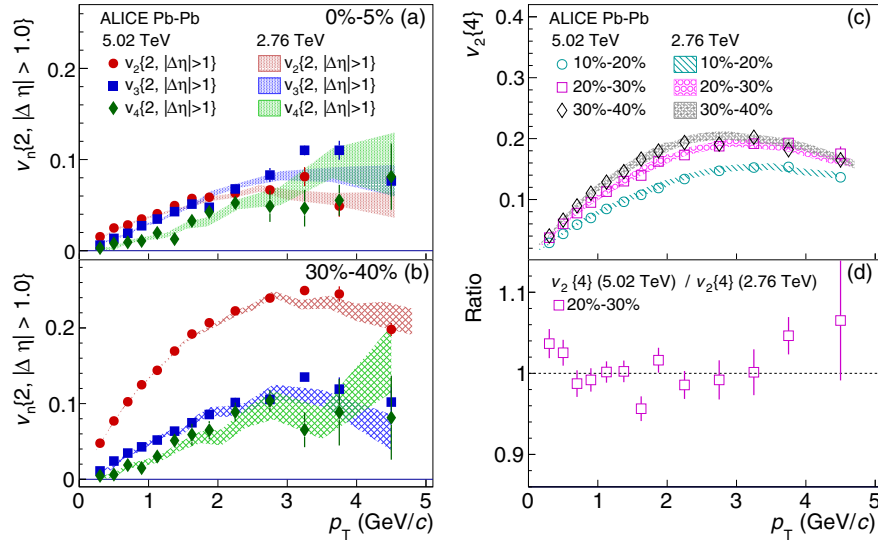
FIG. 2. $v_n(p_T)$ using the two-particle cumulant method with $|\Delta\eta| > 1$ for (a) 0%–5% and (b) 30%–40% centrality classes; (c) $v_2(p_T)$ using four-particle cumulant method for the centrality 10%–20%, 20%–30%, and 30%–40%. Measurements for Pb-Pb collisions at $\sqrt{s_{NN}} = 2.76$ TeV are also presented as shading. (d) The ratio of $v_2\{4\}$ in 20%–30% from two collision energies is also shown here. The statistical and systematical uncertainties are summed in quadrature (the systematic uncertainty is smaller than the statistical uncertainty, which is typically within 5%).

increase significantly with respect to Pb-Pb collisions at $\sqrt{s_{NN}} = 2.76$ TeV.

The anisotropic flow coefficients $v_2\{2, |\Delta\eta| > 1\}$, $v_3\{2, |\Delta\eta| > 1\}$, and $v_4\{2, |\Delta\eta| > 1\}$ as a function of transverse momentum (p_T) are presented in Fig. 2 for the 0%–5% and 30%–40% centrality classes. For the 0%–5% centrality class, at $p_T > 2\,\mathrm{GeV}/c$ $v_3\{2\}$ is observed to become larger than $v_2\{2\}$, while $v_4\{2\}$ is compatible with $v_2\{2\}$, within uncertainties. For the 30%–40% centrality class, we see that $v_2\{2\}$ is higher than $v_3\{2\}$ and $v_4\{2\}$ for the entire p_T range measured, with no crossing of the different order flow coefficients observed. Figure 2(c) presents the p_T differential $v_2\{4\}$ for the 10%–20%, 20%–30% and 30%–40% centrality classes. The $v_2\{4\}$ decreases from midcentral to central collisions over the p_T range measured. The comparison with the corresponding measurements from Pb-Pb collisions at $\sqrt{s_{NN}} = 2.76$ TeV exhibits comparable values, as illustrated by the ratio of $v_2\{4\}$ for the two energies in Fig. 2(d). This indicates that the increase observed in the p_T integrated flow results seen in Fig. 1 can be attributed to an increase of mean transverse momentum $\langle p_T \rangle$. The measurements of p_T-differential flow are more sensitive to initial conditions and η/s, and they are expected to provide important information to constrain further details of the theoretical calculations, e.g., determination of radial flow and freeze-out conditions.

Figure 3 presents the comparison of the fully p_T integrated v_2 measured in the 20%–30% centrality in Pb-Pb collisions at the LHC with results at lower energies. This integrated value in the full p_T range is determined using two methods. The first uses fits to the efficiency-

corrected charged-particle spectra and the p_T differential $v_2\{4\}$ presented in Fig. 2, extrapolated to $p_T = 0$. The error on the integrated v_2 is estimated both from the uncertainty on the p_T-differential measurements and from different parametrizations that provide a good fit of the data. The second calculates $v_2\{4\}$ using tracklets formed from SPD hits in the ITS, which have an acceptance of $p_T \gtrsim 50\,\mathrm{MeV}/c$. As each method uses different ALICE subdetectors, they can provide independent measurements of v_2 coefficients. For this centrality range, they agree within 1% for both energies. The values presented in the
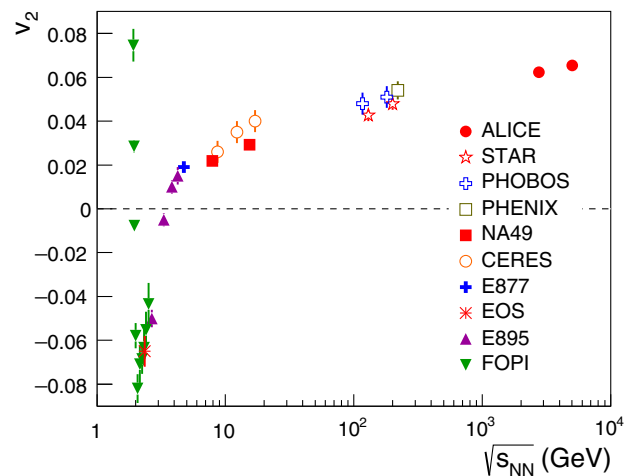

FIG. 3. Integrated elliptic flow ($v_2\{4\}$) for the 20%–30% most central Pb-Pb collisions at $\sqrt{s_{NN}} = 5.02$ TeV compared with v_2 measurements at lower energies with similar centralities (see Ref. [13] for references to all data points).

figure are weighted averages of these two measurements, using the inverse of the variance of each of them as weights. A continuous increase of anisotropic flow for this centrality has been observed from SPS and RHIC to LHC energies. For these fully p_T integrated coefficients, an increase of $(4.9 \pm 1.9)\%$ is observed going from $\sqrt{s_{NN}} = 2.76$ to 5.02 TeV, which is close to the values of the previously mentioned hydrodynamic calculations [25,27].

In summary, we have presented the first anisotropic flow measurements of charged particles in Pb-Pb collisions at $\sqrt{s_{NN}} = 5.02$ TeV at the LHC. An average increase of $(3.0 \pm 0.6)\%$, $(4.3 \pm 1.4)\%$, and $(10.2 \pm 3.8)\%$ is observed for the transverse momentum integrated elliptic, triangular, and quadrangular flow, respectively, over the centrality range 0%–50%, going from 2.76 to 5.02 TeV. The transverse momentum dependence of anisotropic flow has also been investigated, and it does not change appreciably between the two LHC energies. Therefore, the increase in integrated flow coefficients can be attributed mostly to an increase in average transverse momentum. The measurements are found to be compatible with predictions from hydrodynamic models [25,27]. Further comparisons of p_T-differential flow measurements and theoretical calculations, which are not available at this time, will provide extra constraints on the initial conditions and the transport properties of the QGP.

[1] S. Borsanyi, G. Endrodi, Z. Fodor, A. Jakovac, S. D. Katz, S. Krieg, C. Ratti, and K. K. Szabo, The QCD equation of state with dynamical quarks, J. High Energy Phys. 11 (2010) 077.

[2] A. Bazavov *et al.* (HotQCD Collaboration), Equation of state in $(2+1)$-flavor QCD, Phys. Rev. D **90**, 094503 (2014).

[3] K. Aamodt *et al.* (ALICE Collaboration), Centrality Dependence of the Charged-Particle Multiplicity Density at Midrapidity in Pb-Pb Collisions at $\sqrt{s_{NN}} = 2.76$ TeV, Phys. Rev. Lett. **106**, 032301 (2011).

[4] J. Adam *et al.* (ALICE Collaboration), Centrality dependence of the charged-particle multiplicity density at mid-rapidity in Pb-Pb collisions at $\sqrt{s_{NN}} = 5.02$ TeV, arXiv:1512.06104.

[5] G. Odyniec, RHIC beam energy scan program: Phase I and II, *Proc. Sci.*, CPOD2013 (2013) 043.

[6] L. Adamczyk *et al.* (STAR Collaboration), Inclusive charged hadron elliptic flow in $Au + Au$ collisions at $\sqrt{s_{NN}} = 7.7$–39 GeV, Phys. Rev. C **86**, 054908 (2012).

[7] S. S. Adler *et al.* (PHENIX Collaboration), Transverse-energy distributions at midrapidity in $p + p$, $d + Au$, and $Au + Au$ collisions at $\sqrt{s_{NN}} = 62.4$–200 GeV and implications for particle-production models, Phys. Rev. C **89**, 044905 (2014).

[8] R. V. Gavai and S. Gupta, On the critical end point of QCD, Phys. Rev. D **71**, 114014 (2005).

[9] P. Braun-Munzinger, V. Koch, T. Schaefer, and J. Stachel, Properties of hot and dense matter from relativistic heavy ion collisions, Phys. Rept. **621** 76 (2016).

[10] J.-Y. Ollitrault, Anisotropy as a signature of transverse collective flow, Phys. Rev. D **46**, 229 (1992).

[11] S. A. Voloshin, A. M. Poskanzer, and R. Snellings, in *Relativistic Heavy Ion Physics*, edited by Landolt-Boernstein, Vol. 1/23, pp. 5–54 (Springer-Verlag, 2010).

[12] S. Voloshin and Y. Zhang, Flow study in relativistic nuclear collisions by Fourier expansion of Azimuthal particle distributions, Z. Phys. C **70**, 665 (1996).

[13] K. Aamodt *et al.* (ALICE Collaboration), Elliptic Flow of Charged Particles in Pb-Pb Collisions at $\sqrt{S_{NN}} = 2.76$ Tev, Phys. Rev. Lett. **105**, 252302 (2010).

[14] K. H. Ackermann *et al.* (STAR Collaboration), Elliptic Flow in $Au + Au$ Collisions at $\sqrt{s_{NN}} = 130$ GeV, Phys. Rev. Lett. **86**, 402 (2001).

[15] M. Luzum and P. Romatschke, Viscous Hydrodynamic Predictions for Nuclear Collisions at the LHC, Phys. Rev. Lett. **103**, 262302 (2009).

[16] T. Hirano, P. Huovinen, and Y. Nara, Elliptic flow in $U + U$ collisions at $\sqrt{s_{NN}} = 200$ GeV and in $Pb + Pb$ collisions at $\sqrt{s_{NN}} = 2.76$ TeV: Prediction from a hybrid approach, Phys. Rev. C **83**, 021902 (2011).

[17] T. Hirano, U. W. Heinz, D. Kharzeev, R. Lacey, and Y. Nara, Hadronic dissipative effects on elliptic flow in ultrarelativistic heavy-ion collisions, Phys. Lett. B **636**, 299 (2006).

[18] H.-J. Drescher, A. Dumitru, and J.-Y. Ollitrault, The centrality dependence of elliptic flow at LHC, J. Phys. G **35**, 054001 (2008).

[19] B. Alver and G. Roland, Collision geometry fluctuations and triangular flow in heavy-ion collisions, Phys. Rev. C **81**, 054905 (2010); **82**, 039903(E) (2010).

[20] K. Aamodt *et al.* (ALICE Collaboration), Higher Harmonic Anisotropic Flow Measurements of Charged Particles in Pb-Pb Collisions at $\sqrt{s_{NN}} = 2.76$ TeV, Phys. Rev. Lett. **107**, 032301 (2011).

[21] G. Aad *et al.* (ATLAS Collaboration), Measurement of the azimuthal anisotropy for charged particle production in $\sqrt{s_{NN}} = 2.76$ TeV lead-lead collisions with the ATLAS detector, Phys. Rev. C **86**, 014907 (2012).

[22] S. Chatrchyan *et al.* (CMS Collaboration), Measurement of higher-order harmonic azimuthal anisotropy in Pb-Pb collisions at $\sqrt{s_{NN}} = 2.76$ TeV, Phys. Rev. C **89**, 044906 (2014).

[23] G. Aad *et al.* (ATLAS Collaboration), Measurement of event-plane correlations in $\sqrt{s_{NN}} = 2.76$ TeV lead-lead collisions with the ATLAS detector, Phys. Rev. C **90**, 024905 (2014).

[24] P. Kovtun, D. T. Son, and A. O. Starinets, Viscosity in Strongly Interacting Quantum Field Theories from Black Hole Physics, Phys. Rev. Lett. **94**, 111601 (2005).

[25] H. Niemi, K. J. Eskola, R. Paatelainen, and K. Tuominen, Predictions for 5.023 TeV $Pb + Pb$ collisions at the LHC, Phys. Rev. C **93**, 014912 (2016).

[26] N. Borghini, P. M. Dinh, and J.-Y. Ollitrault, New method for measuring azimuthal distributions in nucleus-nucleus collisions, Phys. Rev. C **63**, 054906 (2001).

[27] J. Noronha-Hostler, M. Luzum, and J.-Y. Ollitrault, Hydrodynamic predictions for 5.02 TeV Pb-Pb collisions, Phys. Rev. C **93**, 034912 (2016).

[28] C. Shen and U. Heinz, Collision energy dependence of viscous hydrodynamic flow in relativistic heavy-ion collisions, Phys. Rev. C **85**, 054902 (2012); **86**, 049903(E) (2012).

[29] J. Auvinen and H. Petersen, Evolution of elliptic and triangular flow as a function of beam energy in a hybrid model, J. Phys. Conf. Ser. **503**, 012025 (2014).

[30] K. Aamodt *et al.* (ALICE Collaboration), The ALICE experiment at the CERN LHC, J. Instrum. **3**, S08002 (2008).

[31] P. Cortese *et al.* (ALICE Collaboration), ALICE: Physics performance report, volume II, J. Phys. G **32**, 1295 (2006).

[32] B. Abelev *et al.* (ALICE Collaboration), Centrality determination of Pb-Pb collisions at $\sqrt{s_{NN}} = 2.76$ TeV with ALICE, Phys. Rev. C **88**, 044909 (2013).

[33] X.-N. Wang and M. Gyulassy, HIJING: A Monte Carlo model for multiple jet production in pp, pA and AA collisions, Phys. Rev. D **44**, 3501 (1991).

[34] R. Brun, F. Carminati, and S. Giani, Report No. CERN-W5013, 1994.

[35] Y. Zhou, X. Zhu, P. Li, and H. Song, Investigation of possible hadronic flow in $\sqrt{s_{NN}} = 5.02$ TeV p–Pb collisions, Phys. Rev. C **91**, 064908 (2015).

[36] A. Bilandzic, R. Snellings, and S. Voloshin, Flow analysis with cumulants: Direct calculations, Phys. Rev. C **83**, 044913 (2011).

[37] A. Bilandzic, C. H. Christensen, K. Gulbrandsen, A. Hansen, and Y. Zhou, Generic framework for anisotropic flow analyses with multiparticle azimuthal correlations, Phys. Rev. C **89**, 064904 (2014).

[38] B. B. Abelev *et al.* (ALICE Collaboration), Multiparticle azimuthal correlations in p-Pb and Pb-Pb collisions at the CERN Large Hadron Collider, Phys. Rev. C **90**, 054901 (2014).

J. Adam,[39] D. Adamová,[84] M. M. Aggarwal,[88] G. Aglieri Rinella,[35] M. Agnello,[110] N. Agrawal,[47] Z. Ahammed,[132] S. Ahmad,[19] S. U. Ahn,[68] S. Aiola,[136] A. Akindinov,[58] S. N. Alam,[132] D. S. D. Albuquerque,[121] D. Aleksandrov,[80] B. Alessandro,[110] D. Alexandre,[101] R. Alfaro Molina,[64] A. Alici,[104,12] A. Alkin,[3] J. R. M. Almaraz,[119] J. Alme,[37] T. Alt,[42] S. Altinpinar,[18] I. Altsybeev,[131] C. Alves Garcia Prado,[120] C. Andrei,[78] A. Andronic,[97] V. Anguelov,[94] T. Antičić,[98] F. Antinori,[107] P. Antonioli,[104] L. Aphecetche,[113] H. Appelshäuser,[53] S. Arcelli,[27] R. Arnaldi,[110] O. W. Arnold,[36,93] I. C. Arsene,[22] M. Arslandok,[53] B. Audurier,[113] A. Augustinus,[35] R. Averbeck,[97] M. D. Azmi,[19] A. Badalà,[106] Y. W. Baek,[67] S. Bagnasco,[110] R. Bailhache,[53] R. Bala,[91] S. Balasubramanian,[136] A. Baldisseri,[15] R. C. Baral,[61] A. M. Barbano,[26] R. Barbera,[28] F. Barile,[32] G. G. Barnaföldi,[135] L. S. Barnby,[101] V. Barret,[70] P. Bartalini,[7] K. Barth,[35] J. Bartke,[117] E. Bartsch,[53] M. Basile,[27] N. Bastid,[70] S. Basu,[132] B. Bathen,[54] G. Batigne,[113] A. Batista Camejo,[70] B. Batyunya,[66] P. C. Batzing,[22] I. G. Bearden,[81] H. Beck,[53] C. Bedda,[110] N. K. Behera,[50,48] I. Belikov,[55] F. Bellini,[27] H. Bello Martinez,[2] R. Bellwied,[122] R. Belmont,[134] E. Belmont-Moreno,[64] V. Belyaev,[75] P. Benacek,[84] G. Bencedi,[135] S. Beole,[26] I. Berceanu,[78] A. Bercuci,[78] Y. Berdnikov,[86] D. Berenyi,[135] R. A. Bertens,[57] D. Berzano,[35] L. Betev,[35] A. Bhasin,[91] I. R. Bhat,[91] A. K. Bhati,[88] B. Bhattacharjee,[44] J. Bhom,[128,117] L. Bianchi,[122] N. Bianchi,[72] C. Bianchin,[134] J. Bielčík,[39] J. Bielčíková,[84] A. Bilandzic,[81,36,93] G. Biro,[135] R. Biswas,[4] S. Biswas,[4,79] S. Bjelogrlic,[57] J. T. Blair,[118] D. Blau,[80] C. Blume,[53] F. Bock,[74,94] A. Bogdanov,[75] H. Bøggild,[81] L. Boldizsár,[135] M. Bombara,[40] J. Book,[53] H. Borel,[15] A. Borissov,[96] M. Borri,[83,124] F. Bossú,[65] E. Botta,[26] C. Bourjau,[81] P. Braun-Munzinger,[97] M. Bregant,[120] T. Breitner,[52] T. A. Broker,[53] T. A. Browning,[95] M. Broz,[39] E. J. Brucken,[45] E. Bruna,[110] G. E. Bruno,[32] D. Budnikov,[99] H. Buesching,[53] S. Bufalino,[35,26] P. Buncic,[35] O. Busch,[94,128] Z. Buthelezi,[65] J. B. Butt,[16] J. T. Buxton,[20] J. Cabala,[115] D. Caffarri,[35] X. Cai,[7] H. Caines,[136] L. Calero Diaz,[72] A. Caliva,[57] E. Calvo Villar,[102] P. Camerini,[25] F. Carena,[35] W. Carena,[35] F. Carnesecchi,[27] J. Castillo Castellanos,[15] A. J. Castro,[125] E. A. R. Casula,[24] C. Ceballos Sanchez,[9] J. Cepila,[39] P. Cerello,[110] J. Cerkala,[115] B. Chang,[123] S. Chapeland,[35] M. Chartier,[124] J. L. Charvet,[15] S. Chattopadhyay,[132] S. Chattopadhyay,[100] A. Chauvin,[93,36] V. Chelnokov,[3] M. Cherney,[87] C. Cheshkov,[130] B. Cheynis,[130] V. Chibante Barroso,[35] D. D. Chinellato,[121] S. Cho,[50] P. Chochula,[35] K. Choi,[96] M. Chojnacki,[81] S. Choudhury,[132] P. Christakoglou,[82] C. H. Christensen,[81] P. Christiansen,[33] T. Chujo,[128] S. U. Chung,[96] C. Cicalo,[105] L. Cifarelli,[12,27] F. Cindolo,[104] J. Cleymans,[90] F. Colamaria,[32] D. Colella,[59,35] A. Collu,[74,24] M. Colocci,[27] G. Conesa Balbastre,[71] Z. Conesa del Valle,[51] M. E. Connors,[136,a] J. G. Contreras,[39] T. M. Cormier,[85] Y. Corrales Morales,[110] I. Cortés Maldonado,[2] P. Cortese,[31] M. R. Cosentino,[120] F. Costa,[35] P. Crochet,[70] R. Cruz Albino,[11] E. Cuautle,[63] L. Cunqueiro,[54,35] T. Dahms,[93,36] A. Dainese,[107] M. C. Danisch,[94] A. Danu,[62] D. Das,[100] I. Das,[100] S. Das,[4] A. Dash,[79] S. Dash,[47] S. De,[120] A. De Caro,[12,30] G. de Cataldo,[103] C. de Conti,[120] J. de Cuveland,[42] A. De Falco,[24] D. De Gruttola,[12,30] N. De Marco,[110] S. De Pasquale,[30] A. Deisting,[97,94] A. Deloff,[77] E. Dénes,[135,†] C. Deplano,[82] P. Dhankher,[47] D. Di Bari,[32] A. Di Mauro,[35] P. Di Nezza,[72] M. A. Diaz Corchero,[10] T. Dietel,[90] P. Dillenseger,[53] R. Divià,[35] Ø. Djuvsland,[18] A. Dobrin,[82,62] D. Domenicis Gimenez,[120] B. Dönigus,[53] O. Dordic,[22] T. Drozhzhova,[53] A. K. Dubey,[132] A. Dubla,[57] L. Ducroux,[130] P. Dupieux,[70] R. J. Ehlers,[136] D. Elia,[103] E. Endress,[102] H. Engel,[52] E. Epple,[136] B. Erazmus,[113] I. Erdemir,[53] F. Erhardt,[129] B. Espagnon,[51] M. Estienne,[113] S. Esumi,[128] J. Eum,[96] D. Evans,[101] S. Evdokimov,[111] G. Eyyubova,[39] L. Fabbietti,[93,36] D. Fabris,[107] J. Faivre,[71] A. Fantoni,[72] M. Fasel,[74] L. Feldkamp,[54] A. Feliciello,[110] G. Feofilov,[131] J. Ferencei,[84] A. Fernández Téllez,[2] E. G. Ferreiro,[17] A. Ferretti,[26] A. Festanti,[29] V. J. G. Feuillard,[15,70] J. Figiel,[117] M. A. S. Figueredo,[124,120] S. Filchagin,[99] D. Finogeev,[56] F. M. Fionda,[24] E. M. Fiore,[32] M. G. Fleck,[94] M. Floris,[35] S. Foertsch,[65] P. Foka,[97] S. Fokin,[80] E. Fragiacomo,[109] A. Francescon,[35,29] U. Frankenfeld,[97] G. G. Fronze,[26] U. Fuchs,[35] C. Furget,[71] A. Furs,[56] M. Fusco Girard,[30] J. J. Gaardhøje,[81] M. Gagliardi,[26] A. M. Gago,[102] M. Gallio,[26] D. R. Gangadharan,[74] P. Ganoti,[89] C. Gao,[7] C. Garabatos,[97] E. Garcia-Solis,[13] C. Gargiulo,[35] P. Gasik,[93,36] E. F. Gauger,[118] M. Germain,[113] A. Gheata,[35] M. Gheata,[35,62] P. Ghosh,[132] S. K. Ghosh,[4] P. Gianotti,[72] P. Giubellino,[110,35] P. Giubilato,[29] E. Gladysz-Dziadus,[117] P. Glässel,[94] D. M. Gómez Coral,[64] A. Gomez Ramirez,[52] A. S. Gonzalez,[35] V. Gonzalez,[10] P. González-Zamora,[10] S. Gorbunov,[42] L. Görlich,[117] S. Gotovac,[116] V. Grabski,[64] O. A. Grachov,[136] L. K. Graczykowski,[133] K. L. Graham,[101] A. Grelli,[57] A. Grigoras,[35] C. Grigoras,[35] V. Grigoriev,[75] A. Grigoryan,[1] S. Grigoryan,[66] B. Grinyov,[3] N. Grion,[109] J. M. Gronefeld,[97] J. F. Grosse-Oetringhaus,[35] R. Grosso,[97] F. Guber,[56] R. Guernane,[71] B. Guerzoni,[27] K. Gulbrandsen,[81] T. Gunji,[127] A. Gupta,[91] R. Gupta,[91] R. Haake,[54] Ø. Haaland,[18] C. Hadjidakis,[51] M. Haiduc,[62] H. Hamagaki,[127] G. Hamar,[135] J. C. Hamon,[55] J. W. Harris,[136] A. Harton,[13] D. Hatzifotiadou,[104] S. Hayashi,[127] S. T. Heckel,[53] E. Hellbär,[53] H. Helstrup,[37] A. Herghelegiu,[78] G. Herrera Corral,[11] B. A. Hess,[34] K. F. Hetland,[37] H. Hillemanns,[35] B. Hippolyte,[55] D. Horak,[39] R. Hosokawa,[128] P. Hristov,[35] T. J. Humanic,[20] N. Hussain,[44] T. Hussain,[19] D. Hutter,[42] D. S. Hwang,[21] R. Ilkaev,[99] M. Inaba,[128] E. Incani,[24] M. Ippolitov,[75,80] M. Irfan,[19] M. Ivanov,[97] V. Ivanov,[86]

V. Izucheev,[111] N. Jacazio,[27] P. M. Jacobs,[74] M. B. Jadhav,[47] S. Jadlovska,[115] J. Jadlovsky,[115,59] C. Jahnke,[120] M. J. Jakubowska,[133] H. J. Jang,[68] M. A. Janik,[133] P. H. S. Y. Jayarathna,[122] C. Jena,[29] S. Jena,[122] R. T. Jimenez Bustamante,[97] P. G. Jones,[101] A. Jusko,[101] P. Kalinak,[59] A. Kalweit,[35] J. Kamin,[53] J. H. Kang,[137] V. Kaplin,[75] S. Kar,[132] A. Karasu Uysal,[69] O. Karavichev,[56] T. Karavicheva,[56] L. Karayan,[97,94] E. Karpechev,[56] U. Kebschull,[52] R. Keidel,[138] D. L. D. Keijdener,[57] M. Keil,[35] M. Mohisin Khan,[19,b] P. Khan,[100] S. A. Khan,[132] A. Khanzadeev,[86] Y. Kharlov,[111] B. Kileng,[37] D. W. Kim,[43] D. J. Kim,[123] D. Kim,[137] H. Kim,[137] J. S. Kim,[43] M. Kim,[137] S. Kim,[21] T. Kim,[137] S. Kirsch,[42] I. Kisel,[42] S. Kiselev,[58] A. Kisel,[133] G. Kiss,[135] J. L. Klay,[6] C. Klein,[53] J. Klein,[35] C. Klein-Bösing,[54] S. Klewin,[94] A. Kluge,[35] M. L. Knichel,[94] A. G. Knospe,[118,122] C. Kobdaj,[114] M. Kofarago,[35] T. Kollegger,[97] A. Kolojvari,[131] V. Kondratiev,[131] N. Kondratyeva,[75] E. Kondratyuk,[111] A. Konevskikh,[56] M. Kopcik,[115] P. Kostarakis,[89] M. Kour,[91] C. Kouzinopoulos,[35] O. Kovalenko,[77] V. Kovalenko,[131] M. Kowalski,[117] G. Koyithatta Meethaleveedu,[47] I. Králik,[59] A. Kravčáková,[40] M. Krivda,[59,101] F. Krizek,[84] E. Kryshen,[86,35] M. Krzewicki,[42] A. M. Kubera,[20] V. Kučera,[84] C. Kuhn,[55] P. G. Kuijer,[82] A. Kumar,[91] J. Kumar,[47] L. Kumar,[88] S. Kumar,[47] P. Kurashvili,[77] A. Kurepin,[56] A. B. Kurepin,[56] A. Kuryakin,[99] M. J. Kweon,[50] Y. Kwon,[137] S. L. La Pointe,[110] P. La Rocca,[28] P. Ladron de Guevara,[11] C. Lagana Fernandes,[120] I. Lakomov,[35] R. Langoy,[41] C. Lara,[52] A. Lardeux,[15] A. Lattuca,[26] E. Laudi,[35] R. Lea,[25] L. Leardini,[94] G. R. Lee,[101] S. Lee,[137] F. Lehas,[82] R. C. Lemmon,[83] V. Lenti,[103] E. Leogrande,[57] I. León Monzón,[119] H. León Vargas,[64] M. Leoncino,[26] P. Lévai,[135] S. Li,[7,70] X. Li,[14] J. Lien,[41] R. Lietava,[101] S. Lindal,[22] V. Lindenstruth,[42] C. Lippmann,[97] M. A. Lisa,[20] H. M. Ljunggren,[33] D. F. Lodato,[57] P. I. Loenne,[18] V. Loginov,[75] C. Loizides,[74] X. Lopez,[70] E. López Torres,[9] A. Lowe,[135] P. Luettig,[53] M. Lunardon,[29] G. Luparello,[25] T. H. Lutz,[136] A. Maevskaya,[56] M. Mager,[35] S. Mahajan,[91] S. M. Mahmood,[22] A. Maire,[55] R. D. Majka,[136] M. Malaev,[86] I. Maldonado Cervantes,[63] L. Malinina,[66,c] D. Mal'Kevich,[58] P. Malzacher,[97] A. Mamonov,[99] V. Manko,[80] F. Manso,[70] V. Manzari,[103,35] M. Marchisone,[65,126,26] J. Mareš,[60] G. V. Margagliotti,[25] A. Margotti,[104] J. Margutti,[57] A. Marín,[97] C. Markert,[118] M. Marquard,[53] N. A. Martin,[97] J. Martin Blanco,[113] P. Martinengo,[35] M. I. Martínez,[2] G. Martínez García,[113] M. Martinez Pedreira,[35] A. Mas,[120] S. Masciocchi,[97] M. Masera,[26] A. Masoni,[105] A. Mastroserio,[32] A. Matyja,[117] C. Mayer,[117] J. Mazer,[125] M. A. Mazzoni,[108] D. Mcdonald,[122] F. Meddi,[23] Y. Melikyan,[75] A. Menchaca-Rocha,[64] E. Meninno,[30] J. Mercado Pérez,[94] M. Meres,[38] Y. Miake,[128] M. M. Mieskolainen,[45] K. Mikhaylov,[66,58] L. Milano,[35,74] J. Milosevic,[22] A. Mischke,[57] A. N. Mishra,[48] D. Miśkowiec,[97] J. Mitra,[132] C. M. Mitu,[62] N. Mohammadi,[57] B. Mohanty,[132,79] L. Molnar,[55,113] L. Montaño Zetina,[11] E. Montes,[10] D. A. Moreira De Godoy,[54] L. A. P. Moreno,[2] S. Moretto,[29] A. Morreale,[113] A. Morsch,[35] V. Muccifora,[72] E. Mudnic,[116] D. Mühlheim,[54] S. Muhuri,[132] M. Mukherjee,[132] J. D. Mulligan,[136] M. G. Munhoz,[120] R. H. Munzer,[93,36,53] H. Murakami,[127] S. Murray,[65] L. Musa,[35] J. Musinsky,[59] B. Naik,[47] R. Nair,[77] B. K. Nandi,[47] R. Nania,[104] E. Nappi,[103] M. U. Naru,[16] H. Natal da Luz,[120] C. Nattrass,[125] S. R. Navarro,[2] K. Nayak,[79] R. Nayak,[47] T. K. Nayak,[132] S. Nazarenko,[99] A. Nedosekin,[58] L. Nellen,[63] F. Ng,[122] M. Nicassio,[97] M. Niculescu,[62] J. Niedziela,[35] B. S. Nielsen,[81] S. Nikolaev,[80] S. Nikulin,[80] V. Nikulin,[86] F. Noferini,[104,12] P. Nomokonov,[66] G. Nooren,[57] J. C. C. Noris,[2] J. Norman,[124] A. Nyanin,[80] J. Nystrand,[18] H. Oeschler,[94] S. Oh,[136] S. K. Oh,[67] A. Ohlson,[35] A. Okatan,[69] T. Okubo,[46] L. Olah,[135] J. Oleniacz,[133] A. C. Oliveira Da Silva,[120] M. H. Oliver,[136] J. Onderwaater,[97] C. Oppedisano,[110] R. Orava,[45] M. Oravec,[115] A. Ortiz Velasquez,[63] A. Oskarsson,[33] J. Otwinowski,[117] K. Oyama,[94,76] M. Ozdemir,[53] Y. Pachmayer,[94] D. Pagano,[26] P. Pagano,[30] G. Paić,[63] S. K. Pal,[132] J. Pan,[134] A. K. Pandey,[47] V. Papikyan,[1] G. S. Pappalardo,[106] P. Pareek,[48] W. J. Park,[97] S. Parmar,[88] A. Passfeld,[54] V. Paticchio,[103] R. N. Patra,[132] B. Paul,[100] H. Pei,[7] T. Peitzmann,[57] H. Pereira Da Costa,[15] D. Peresunko,[80,75] C. E. Pérez Lara,[82] E. Perez Lezama,[53] V. Peskov,[53] Y. Pestov,[5] V. Petráček,[39] V. Petrov,[111] M. Petrovici,[78] C. Petta,[28] S. Piano,[109] M. Pikna,[38] P. Pillot,[113] L. O. D. L. Pimentel,[81] O. Pinazza,[104,35] L. Pinsky,[122] D. B. Piyarathna,[122] M. Płoskoń,[74] M. Planinic,[129] J. Pluta,[133] S. Pochybova,[135] P. L. M. Podesta-Lerma,[119] M. G. Poghosyan,[85,87] B. Polichtchouk,[111] N. Poljak,[129] W. Poonsawat,[114] A. Pop,[78] S. Porteboeuf-Houssais,[70] J. Porter,[74] J. Pospisil,[84] S. K. Prasad,[4] R. Preghenella,[104,35] F. Prino,[110] C. A. Pruneau,[134] I. Pshenichnov,[56] M. Puccio,[26] G. Puddu,[24] P. Pujahari,[134] V. Punin,[99] J. Putschke,[134] H. Qvigstad,[22] A. Rachevski,[109] S. Raha,[4] S. Rajput,[91] J. Rak,[123] A. Rakotozafindrabe,[15] L. Ramello,[31] F. Rami,[55] R. Raniwala,[92] S. Raniwala,[92] S. S. Räsänen,[45] B. T. Rascanu,[53] D. Rathee,[88] K. F. Read,[85,125] K. Redlich,[77] R. J. Reed,[134] A. Rehman,[18] P. Reichelt,[53] F. Reidt,[94,35] X. Ren,[7] R. Renfordt,[53] A. R. Reolon,[72] A. Reshetin,[56] K. Reygers,[94] V. Riabov,[86] R. A. Ricci,[73] T. Richert,[33] M. Richter,[22] P. Riedler,[35] W. Riegler,[35] F. Riggi,[28] C. Ristea,[62] E. Rocco,[57] M. Rodríguez Cahuantzi,[11,2] A. Rodriguez Manso,[82] K. Røed,[22] E. Rogochaya,[66] D. Rohr,[42] D. Röhrich,[18] F. Ronchetti,[72,35] L. Ronflette,[113] P. Rosnet,[70] A. Rossi,[35,29] F. Roukoutakis,[89] A. Roy,[48] C. Roy,[55] P. Roy,[100] A. J. Rubio Montero,[10] R. Rui,[25] R. Russo,[26] E. Ryabinkin,[80] Y. Ryabov,[86] A. Rybicki,[117] S. Saarinen,[45] S. Sadhu,[132]

S. Sadovsky,[111] K. Šafařík,[35] B. Sahlmuller,[53] P. Sahoo,[48] R. Sahoo,[48] S. Sahoo,[61] P. K. Sahu,[61] J. Saini,[132] S. Sakai,[74] M. A. Saleh,[134] J. Salzwedel,[20] S. Sambyal,[91] V. Samsonov,[86] L. Šándor,[59] A. Sandoval,[64] M. Sano,[128] D. Sarkar,[132] N. Sarkar,[132] P. Sarma,[44] E. Scapparone,[104] F. Scarlassara,[29] C. Schiaua,[78] R. Schicker,[94] C. Schmidt,[97] H. R. Schmidt,[34] S. Schuchmann,[53] J. Schukraft,[35] M. Schulc,[39] Y. Schutz,[35,113] K. Schwarz,[97] K. Schweda,[97] G. Scioli,[27] E. Scomparin,[110] R. Scott,[125] M. Šefčík,[40] J. E. Seger,[87] Y. Sekiguchi,[127] D. Sekihata,[46] I. Selyuzhenkov,[97] K. Senosi,[65] S. Senyukov,[3,35] E. Serradilla,[10,64] A. Sevcenco,[62] A. Shabanov,[56] A. Shabetai,[113] O. Shadura,[3] R. Shahoyan,[35] M. I. Shahzad,[16] A. Shangaraev,[111] A. Sharma,[91] M. Sharma,[91] M. Sharma,[91] N. Sharma,[125] A. I. Sheikh,[132] K. Shigaki,[46] Q. Shou,[7] K. Shtejer,[26,9] Y. Sibiriak,[80] S. Siddhanta,[105] K. M. Sielewicz,[35] T. Siemiarczuk,[77] D. Silvermyr,[33] C. Silvestre,[71] G. Simatovic,[129] G. Simonetti,[35] R. Singaraju,[132] R. Singh,[79] S. Singha,[132,79] V. Singhal,[132] B. C. Sinha,[132] T. Sinha,[100] B. Sitar,[38] M. Sitta,[31] T. B. Skaali,[22] M. Slupecki,[123] N. Smirnov,[136] R. J. M. Snellings,[57] T. W. Snellman,[123] J. Song,[96] M. Song,[137] Z. Song,[7] F. Soramel,[29] S. Sorensen,[125] R. D. de Souza,[121] F. Sozzi,[97] M. Spacek,[39] E. Spiriti,[72] I. Sputowska,[117] M. Spyropoulou-Stassinaki,[89] J. Stachel,[94] I. Stan,[62] P. Stankus,[85] E. Stenlund,[33] G. Steyn,[65] J. H. Stiller,[94] D. Stocco,[113] P. Strmen,[38] A. A. P. Suaide,[120] T. Sugitate,[46] C. Suire,[51] M. Suleymanov,[16] M. Suljic,[25,†] R. Sultanov,[58] M. Šumbera,[84] S. Sumowidagdo,[49] A. Szabo,[38] A. Szanto de Toledo,[120,†] I. Szarka,[38] A. Szczepankiewicz,[35] M. Szymanski,[133] U. Tabassam,[16] J. Takahashi,[121] G. J. Tambave,[18] N. Tanaka,[128] M. Tarhini,[51] M. Tariq,[19] M. G. Tarzila,[78] A. Tauro,[35] G. Tejeda Muñoz,[2] A. Telesca,[35] K. Terasaki,[127] C. Terrevoli,[29] B. Teyssier,[130] J. Thäder,[74] D. Thakur,[48] D. Thomas,[118] R. Tieulent,[130] A. R. Timmins,[122] A. Toia,[53] S. Trogolo,[26] G. Trombetta,[32] V. Trubnikov,[3] W. H. Trzaska,[123] T. Tsuji,[127] A. Tumkin,[99] R. Turrisi,[107] T. S. Tveter,[22] K. Ullaland,[18] A. Uras,[130] G. L. Usai,[24] A. Utrobicic,[129] M. Vala,[59] L. Valencia Palomo,[70] S. Vallero,[26] J. Van Der Maarel,[57] J. W. Van Hoorne,[35] M. van Leeuwen,[57] T. Vanat,[84] P. Vande Vyvre,[35] D. Varga,[135] A. Vargas,[2] M. Vargyas,[123] R. Varma,[47] M. Vasileiou,[89] A. Vasiliev,[80] A. Vauthier,[71] V. Vechernin,[131] A. M. Veen,[57] M. Veldhoen,[57] A. Velure,[18] E. Vercellin,[26] S. Vergara Limón,[2] R. Vernet,[8] M. Verweij,[134] L. Vickovic,[116] G. Viesti,[29,†] J. Viinikainen,[123] Z. Vilakazi,[126] O. Villalobos Baillie,[101] A. Villatoro Tello,[2] A. Vinogradov,[80,†] L. Vinogradov,[131] Y. Vinogradov,[99,†] T. Virgili,[30] V. Vislavicius,[33] Y. P. Viyogi,[132] A. Vodopyanov,[66] M. A. Völkl,[94] K. Voloshin,[58] S. A. Voloshin,[134] G. Volpe,[32,135] B. von Haller,[35] I. Vorobyev,[36,93] D. Vranic,[97,35] J. Vrláková,[40] B. Vulpescu,[70] B. Wagner,[18] J. Wagner,[97] H. Wang,[57] M. Wang,[7,113] D. Watanabe,[128] Y. Watanabe,[127] M. Weber,[35,112] S. G. Weber,[97] D. F. Weiser,[94] J. P. Wessels,[54] U. Westerhoff,[54] A. M. Whitehead,[90] J. Wiechula,[34] J. Wikne,[22] G. Wilk,[77] J. Wilkinson,[94] M. C. S. Williams,[104] B. Windelband,[94] M. Winn,[94] H. Yang,[57] P. Yang,[7] S. Yano,[46] Z. Yasin,[16] Z. Yin,[7] H. Yokoyama,[128] I.-K. Yoo,[96] J. H. Yoon,[50] V. Yurchenko,[3] I. Yushmanov,[80] A. Zaborowska,[133] V. Zaccolo,[81] A. Zaman,[16] C. Zampolli,[104,35] H. J. C. Zanoli,[120] S. Zaporozhets,[66] N. Zardoshti,[101] A. Zarochentsev,[131] P. Závada,[60] N. Zaviyalov,[99] H. Zbroszczyk,[133] I. S. Zgura,[62] M. Zhalov,[86] H. Zhang,[18] X. Zhang,[74,7] Y. Zhang,[7] C. Zhang,[57] Z. Zhang,[7] C. Zhao,[22] N. Zhigareva,[58] D. Zhou,[7] Y. Zhou,[81] Z. Zhou,[18] H. Zhu,[18] J. Zhu,[7,113] A. Zichichi,[27,12] A. Zimmermann,[94] M. B. Zimmermann,[54,35] G. Zinovjev,[3] and M. Zyzak[42]

(The ALICE Collaboration)

[1] A.I. Alikhanyan National Science Laboratory (Yerevan Physics Institute) Foundation, Yerevan, Armenia
[2] Benemérita Universidad Autónoma de Puebla, Puebla, Mexico
[3] Bogolyubov Institute for Theoretical Physics, Kiev, Ukraine
[4] Bose Institute, Department of Physics and Centre for Astroparticle Physics and Space Science (CAPSS), Kolkata, India
[5] Budker Institute for Nuclear Physics, Novosibirsk, Russia
[6] California Polytechnic State University, San Luis Obispo, California, USA
[7] Central China Normal University, Wuhan, China
[8] Centre de Calcul de l'IN2P3, Villeurbanne, France
[9] Centro de Aplicaciones Tecnológicas y Desarrollo Nuclear (CEADEN), Havana, Cuba
[10] Centro de Investigaciones Energéticas Medioambientales y Tecnológicas (CIEMAT), Madrid, Spain
[11] Centro de Investigación y de Estudios Avanzados (CINVESTAV), Mexico City and Mérida, Mexico
[12] Centro Fermi—Museo Storico della Fisica e Centro Studi e Ricerche "Enrico Fermi," Rome, Italy
[13] Chicago State University, Chicago, Illinois, USA
[14] China Institute of Atomic Energy, Beijing, China
[15] Commissariat à l'Energie Atomique, IRFU, Saclay, France
[16] COMSATS Institute of Information Technology (CIIT), Islamabad, Pakistan
[17] Departamento de Física de Partículas and IGFAE, Universidad de Santiago de Compostela, Santiago de Compostela, Spain
[18] Department of Physics and Technology, University of Bergen, Bergen, Norway

[19]Department of Physics, Aligarh Muslim University, Aligarh, India

[20]Department of Physics, Ohio State University, Columbus, Ohio, USA

[21]Department of Physics, Sejong University, Seoul, South Korea

[22]Department of Physics, University of Oslo, Oslo, Norway

[23]Dipartimento di Fisica dell'Università "La Sapienza" and Sezione INFN Rome, Italy

[24]Dipartimento di Fisica dell'Università and Sezione INFN, Cagliari, Italy

[25]Dipartimento di Fisica dell'Università and Sezione INFN, Trieste, Italy

[26]Dipartimento di Fisica dell'Università and Sezione INFN, Turin, Italy

[27]Dipartimento di Fisica e Astronomia dell'Università and Sezione INFN, Bologna, Italy

[28]Dipartimento di Fisica e Astronomia dell'Università and Sezione INFN, Catania, Italy

[29]Dipartimento di Fisica e Astronomia dell'Università and Sezione INFN, Padova, Italy

[30]Dipartimento di Fisica "E.R. Caianiello" dell'Università and Gruppo Collegato INFN, Salerno, Italy

[31]Dipartimento di Scienze e Innovazione Tecnologica dell'Università del Piemonte Orientale and Gruppo Collegato INFN,
Alessandria, Italy

[32]Dipartimento Interateneo di Fisica "M. Merlin" and Sezione INFN, Bari, Italy

[33]Division of Experimental High Energy Physics, University of Lund, Lund, Sweden

[34]Eberhard Karls Universität Tübingen, Tübingen, Germany

[35]European Organization for Nuclear Research (CERN), Geneva, Switzerland

[36]Excellence Cluster Universe, Technische Universität München, Munich, Germany

[37]Faculty of Engineering, Bergen University College, Bergen, Norway

[38]Faculty of Mathematics, Physics and Informatics, Comenius University, Bratislava, Slovakia

[39]Faculty of Nuclear Sciences and Physical Engineering, Czech Technical University in Prague, Prague, Czech Republic

[40]Faculty of Science, P.J. Šafárik University, Košice, Slovakia

[41]Faculty of Technology, Buskerud and Vestfold University College, Vestfold, Norway

[42]Frankfurt Institute for Advanced Studies, Johann Wolfgang Goethe-Universität Frankfurt, Frankfurt, Germany

[43]Gangneung-Wonju National University, Gangneung, South Korea

[44]Gauhati University, Department of Physics, Guwahati, India

[45]Helsinki Institute of Physics (HIP), Helsinki, Finland

[46]Hiroshima University, Hiroshima, Japan

[47]Indian Institute of Technology Bombay (IIT), Mumbai, India

[48]Indian Institute of Technology Indore, Indore (IITI), India

[49]Indonesian Institute of Sciences, Jakarta, Indonesia

[50]Inha University, Incheon, South Korea

[51]Institut de Physique Nucléaire d'Orsay (IPNO), Université Paris–Sud, CNRS-IN2P3, Orsay, France

[52]Institut für Informatik, Johann Wolfgang Goethe-Universität Frankfurt, Frankfurt, Germany

[53]Institut für Kernphysik, Johann Wolfgang Goethe-Universität Frankfurt, Frankfurt, Germany

[54]Institut für Kernphysik, Westfälische Wilhelms-Universität Münster, Münster, Germany

[55]Institut Pluridisciplinaire Hubert Curien (IPHC), Université de Strasbourg, CNRS-IN2P3, Strasbourg, France

[56]Institute for Nuclear Research, Academy of Sciences, Moscow, Russia

[57]Institute for Subatomic Physics, Utrecht University, Utrecht, Netherlands

[58]Institute for Theoretical and Experimental Physics, Moscow, Russia

[59]Institute of Experimental Physics, Slovak Academy of Sciences, Košice, Slovakia

[60]Institute of Physics, Academy of Sciences of the Czech Republic, Prague, Czech Republic

[61]Institute of Physics, Bhubaneswar, India

[62]Institute of Space Science (ISS), Bucharest, Romania

[63]Instituto de Ciencias Nucleares, Universidad Nacional Autónoma de México, Mexico City, Mexico

[64]Instituto de Física, Universidad Nacional Autónoma de México, Mexico City, Mexico

[65]iThemba LABS, National Research Foundation, Somerset West, South Africa

[66]Joint Institute for Nuclear Research (JINR), Dubna, Russia

[67]Konkuk University, Seoul, South Korea

[68]Korea Institute of Science and Technology Information, Daejeon, South Korea

[69]KTO Karatay University, Konya, Turkey

[70]Laboratoire de Physique Corpusculaire (LPC), Clermont Université, Université Blaise Pascal,
CNRS–IN2P3, Clermont-Ferrand, France

[71]Laboratoire de Physique Subatomique et de Cosmologie, Université Grenoble Alpes, CNRS-IN2P3, Grenoble, France

[72]Laboratori Nazionali di Frascati, INFN, Frascati, Italy

[73]Laboratori Nazionali di Legnaro, INFN, Legnaro, Italy

[74]Lawrence Berkeley National Laboratory, Berkeley, California, USA

[75]Moscow Engineering Physics Institute, Moscow, Russia

[76]Nagasaki Institute of Applied Science, Nagasaki, Japan

[77]National Centre for Nuclear Studies, Warsaw, Poland

[78]National Institute for Physics and Nuclear Engineering, Bucharest, Romania

[79]National Institute of Science Education and Research, Bhubaneswar, India

[80]National Research Centre Kurchatov Institute, Moscow, Russia

[81]Niels Bohr Institute, University of Copenhagen, Copenhagen, Denmark

[82]Nikhef, Nationaal instituut voor subatomaire fysica, Amsterdam, Netherlands

[83]Nuclear Physics Group, STFC Daresbury Laboratory, Daresbury, United Kingdom

[84]Nuclear Physics Institute, Academy of Sciences of the Czech Republic, Řež u Prahy, Czech Republic

[85]Oak Ridge National Laboratory, Oak Ridge, Tennessee, USA

[86]Petersburg Nuclear Physics Institute, Gatchina, Russia

[87]Physics Department, Creighton University, Omaha, Nebraska, USA

[88]Physics Department, Panjab University, Chandigarh, India

[89]Physics Department, University of Athens, Athens, Greece

[90]Physics Department, University of Cape Town, Cape Town, South Africa

[91]Physics Department, University of Jammu, Jammu, India

[92]Physics Department, University of Rajasthan, Jaipur, India

[93]Physik Department, Technische Universität München, Munich, Germany

[94]Physikalisches Institut, Ruprecht-Karls-Universität Heidelberg, Heidelberg, Germany

[95]Purdue University, West Lafayette, Indiana, USA

[96]Pusan National University, Pusan, South Korea

[97]Research Division and ExtreMe Matter Institute EMMI, GSI Helmholtzzentrum für Schwerionenforschung, Darmstadt, Germany

[98]Rudjer Bošković Institute, Zagreb, Croatia

[99]Russian Federal Nuclear Center (VNIIEF), Sarov, Russia

[100]Saha Institute of Nuclear Physics, Kolkata, India

[101]School of Physics and Astronomy, University of Birmingham, Birmingham, United Kingdom

[102]Sección Física, Departamento de Ciencias, Pontificia Universidad Católica del Perú, Lima, Peru

[103]Sezione INFN, Bari, Italy

[104]Sezione INFN, Bologna, Italy

[105]Sezione INFN, Cagliari, Italy

[106]Sezione INFN, Catania, Italy

[107]Sezione INFN, Padova, Italy

[108]Sezione INFN, Rome, Italy

[109]Sezione INFN, Trieste, Italy

[110]Sezione INFN, Turin, Italy

[111]SSC IHEP of NRC Kurchatov institute, Protvino, Russia

[112]Stefan Meyer Institut für Subatomare Physik (SMI), Vienna, Austria

[113]SUBATECH, Ecole des Mines de Nantes, Université de Nantes, CNRS-IN2P3, Nantes, France

[114]Suranaree University of Technology, Nakhon Ratchasima, Thailand

[115]Technical University of Košice, Košice, Slovakia

[116]Technical University of Split FESB, Split, Croatia

[117]The Henryk Niewodniczanski Institute of Nuclear Physics, Polish Academy of Sciences, Cracow, Poland

[118]Physics Department, The University of Texas at Austin, Austin, Texas, USA

[119]Universidad Autónoma de Sinaloa, Culiacán, Mexico

[120]Universidade de São Paulo (USP), São Paulo, Brazil

[121]Universidade Estadual de Campinas (UNICAMP), Campinas, Brazil

[122]University of Houston, Houston, Texas, USA

[123]University of Jyväskylä, Jyväskylä, Finland

[124]University of Liverpool, Liverpool, United Kingdom

[125]University of Tennessee, Knoxville, Tennessee, USA

[126]University of the Witwatersrand, Johannesburg, South Africa

[127]University of Tokyo, Tokyo, Japan

[128]University of Tsukuba, Tsukuba, Japan

[129]University of Zagreb, Zagreb, Croatia

[130]Université de Lyon, Université Lyon 1, CNRS/IN2P3, IPN-Lyon, Villeurbanne, France

[131]V. Fock Institute for Physics, St. Petersburg State University, St. Petersburg, Russia

[132]Variable Energy Cyclotron Centre, Kolkata, India

[133]Warsaw University of Technology, Warsaw, Poland

[134]Wayne State University, Detroit, Michigan, USA

[135]Wigner Research Centre for Physics, Hungarian Academy of Sciences, Budapest, Hungary

[136]Yale University, New Haven, Connecticut, USA

[137]*Yonsei University, Seoul, South Korea*
[138]*Zentrum für Technologietransfer und Telekommunikation (ZTT), Fachhochschule Worms, Worms, Germany*

[†]Deceased.
[a]Also at Georgia State University, Atlanta, Georgia, USA.
[b]Also at Department of Applied Physics, Aligarh Muslim University, Aligarh, India.
[c]Also at D.V. Skobeltsyn Institute of Nuclear Physics, M.V. Lomonosov Moscow State University, Moscow, Russia.